Desirability approach for optimisation of electrothermal atomic absorption spectrometry factors in iron determinations

S. Salomon, P. Giamarchi and A. Le Bihan

UMR 6521, Université de Bretagne Occidentale, 6, avenue Le Gorgeu, 29285 Brest Cedex, France

We report here on iron determination in sea matrix by electrothermal atomic absorption spectrometry. We optimised the experimental conditions of the spectroscopic factors, *i.e.* entrance monochromator slit height, slit width and lamp current, and of the electrothermal factors, *i.e.* calcination temperature, calcination duration, atomisation temperature and injected volume, since these two groups are independent. Because of the technical constraints occurring on our experimental domain of study we built a D-optimal experimental design to conduct these optimisations. We monitored three experimental responses, *i.e.* the standard deviation of the instantaneous specific absorbance, the specific integrated absorbance and the non-specific integrated absorbance. The three of them clearly showed an optimum in three opposed experimental conditions. Consequently, a desirability transformation of the experimental responses permitted us to obtain a better compromise. We, finally, computed a new experimental response which took the raw measurements into account to directly estimate the limits of detection. The optimisation of this computed response showed us that the lowest detection limit was obtained under the same experimental compromise than the one suggested by the desirability study. This result allowed us to validate the computed response as an interesting optimisation criterion in electrothermal atomic absorption spectrometry.

Introduction

In electrothermal atomic absorption spectrometry the optimal operational conditions are specific of each metal and depend on the nature of the sample matrix. Consequently, their determination is difficult. The classical method consisting in changing in turn one of the factors while keeping the others constant is a time-consuming procedure. Numerous applications of experimental design dealing with the determinations of various metals in samples of different nature have been carried out to improve this method. They have used several kinds of experimental design like simplex [1,2], fractional factorial [3,4], central composite [5,6], Doehlert's [7,8] or D-optimal-design; the last one studied a non-classical experimental domain of study [9,10]. Each time the use of experimental design reduced the number of experiments carried out while providing one with more information on each experimental condition tested.

In electrothermal atomic absorption spectrometry the experimental factors can be split into two distinct classes: the spectroscopic factors and the electrothermal ones; they are known as being independent and both need an optimisation of experimental conditions. The study reported here was thus divided into two parts: first, the simultaneous optimisation of the 3 following spectroscopic factors: entrance monochromator slit height, slit width and lamp current, and secondly the simultaneous optimisation of 4 electrothermal factors: calcination temperature, calcination duration, atomisation temperature and injected volume.

The metal of concern in this study was iron in seawater; this matrix is complex because of the high level of dissolved salts inducing interfering phenomena throughout the determination procedure. It thus requires a precise optimisation of the experimental conditions to reach a low iron detection limit.

However, if the application of experimental design is helpful for atomic absorption spectrometry, several experimental responses like, for example, the standard deviation of the instantaneous specific absorbance, the specific and non-specific absorbances need still to be monitored. These responses often differ in their optimal experimental conditions, and the use of desirability approach is liable to bring an interesting answer to this problem.

But, usually spectrometry users are not very familiar with the desirability approach which, moreover, is never proposed in the commercial software supplied with spectroscopy apparatuses. So, to facilitate a direct search of the optimum we found interesting to compute a transformed experimental response that takes into account several experimental responses.

Article available at http://analusis.edpsciences.org or http://dx.doi.org/10.1051/analusis:2000133

Materials and methods

Apparatus and reagents

All atomic absorption spectrometry analyses were carried out on a Varian 880 Z spectrometer with a transverse Zeeman effect correction. The principle of the measurement consisted in introducing a sample of volume *V* (within 10 and 40 µL) into a small graphite furnace. The furnace temperature was then elevated to the calcination temperature *CT;* this increase in temperature was controlled by a precise electrothermal programme selected by the analyst. It also maintained *CT* during the calcination duration *CD* in order to dry and calcinate the sample under a nitrogen gas flow. Then, the sample was heated as quick as possible up to the atomisation temperature *AT* to atomise the metal. These metal vapours were irradiated by a specific hollow cathode lamp (Superlamp Photon) at 248.3 nm. The sample absorbance was recorded versus time (Fig. 1); the integrated absorbance obtained is directly proportional to the metal concentration in the sample.

One should remember that, in electrothermal atomic absorption spectrometry, a systematic difference between two identical and successive measurements can occur; this is caused by unavoidable changes of the graphite furnace surface. Indeed, the spectrometer has been programmed to automatically duplicate all the measurements without any change in experimental conditions. Consequently, the mean of two successive corroborating results is considered as only one experimental response. Despite these cautions, one should be conscious that using the same graphite furnace for more than 60 measurements will induce a non-negligible evolution in the experimental response liable to spoil the measurements by mistakes and lead the analyst to erroneously interpret results.

The samples were prepared in seawater and acidified with 1 % of nitric acid. Iron concentrations were 5 and 1 µg.L^{-1} for the optimisation of spectroscopic factors and electrothermal ones, respectively. During the spectroscopic factors optimisation our knowledge of the spectroscopy technique led us to arbitrarily set the electrothermal factors at the following values: *V* = 10 µL, *CT* = 1700 °C, *CD* = 30 s and *AT* = 2600 °C.

The calculations required for the methodology study were made with the new Windows version of the Nemrod software [11].

Experimental factors and domain of study

To optimise the spectroscopic operational conditions we studied the three following experimental factors denoted S_i:

Spectroscopic factor 1: lamp current denoted S_1 in coded variable or *C* in real variable. By referring to some preliminary studies we set the minimum value to ignite the lamp at 7 mA and the maximum one at 23 mA.

Spectroscopic factor 2: entrance monochromator slit height (S_2 in coded variable or *H* in real variable); it is a qualitative factor with two available positions: normal or reduced. The normal slit allows the entrance of more light than the reduced one and decreases the noise *s*. On the other hand, it may let enter some interfering light from the graphite furnace, whereas a reduced slit limits this problem but results in more noise.

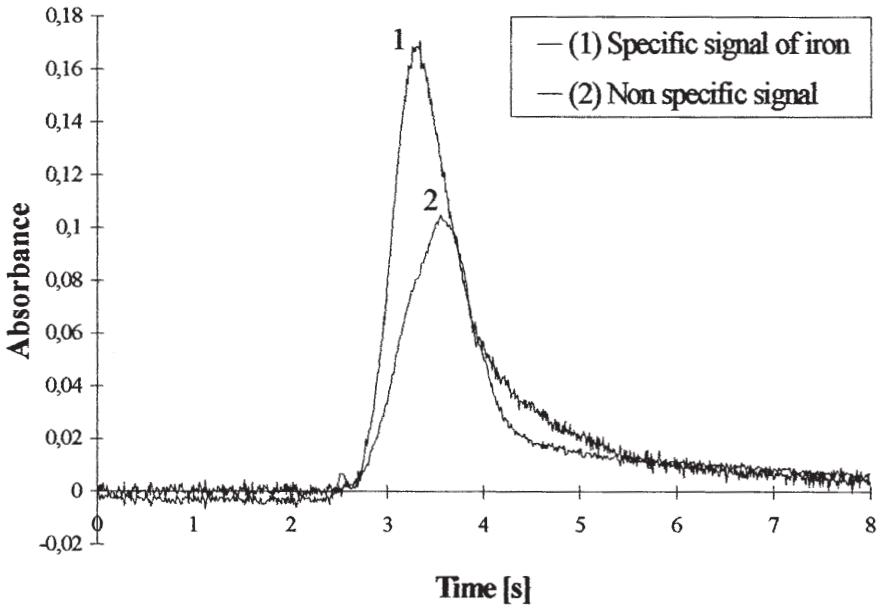

Figure 1. Absorbance signal of atomic absorption spectrometric determination of iron in seawater.

Table I. Levels of study for experimental factors in coded variable, and with their corresponding value in real variable. Part A, for the spectroscopic factors; part B, for the electrothermal factors.

	Real factors names						
	Part A : Spectroscopic factors			*Part B : Electrothermal factors*			
Coded values	*C (mA)*	*H*	*W (nm)*	*V (µL)*	*CT (°C)*	*CD (s)*	*AT (°C)*
1	23	Normal	1	36	1700	50	2700
0	15			24	1600	30	2600
–0.11			0.5				
–0.50						20	
–0.78			0.2				
–1	7	Reduced	0.1	12	1500	10	2500
	S_1	S_2	S_3	E_1	E_2	E_3	E_4
	Coded factors names						

Spectroscopic factor 3: slit width (S_3 in coded variable or *W* in real variable). The slit width value corresponds to the wavelength domain observed by the photomultiplier. Our spectrophotometer imposed us to use only the four following discrete values: 0.1, 0.2, 0.5, and 1 nm, which respectively correspond to the coded values –1, -0.778, -0.111 and 1. As the centre value of $S_3 = 0$ could not be used, there were four possible levels of study for the slit width factor.

All the experimental levels used for the three spectroscopic factors S_i are listed in table I-A.

To optimise the electrothermal operational conditions we decided to study the four following experimental factors denoted E_i:

Electrothermal factor 1: injected volume (E_1 in coded variable or *V* in real variable). An injection of a high volume increases the signal coming from the metal analysed, but increases the non specific absorbance which can create some mathematical miscorrections. To find a compromise we made the volume vary within 12 and 36 µl; indeed these values are the most classical ones and fit well the capability of our apparatus.

Electrothermal factor 2: calcination temperature (E_2 in coded variable or *CT* in real variable). When the temperature is too low, the non-specific signal from other compounds or molecular species than iron can be important; on the other hand, if the temperature is too high iron may be partly lost during the calcination step, which is unacceptable for the analyst. To optimise this factor we studied the temperatures between 1500 to 1700 °C by reference to literature data and to some preliminary trials.

Electrothermal factor 3: calcination duration (E_3 in coded variable or *CD* in real variable). A too short or too long calcination has the same consequences than those mentioned above. By reference to some preliminary trials and to literature data we made it vary between 10 and 50 seconds.

Electrothermal factor 4: atomisation temperature (E_4 in coded variable or *AT* in real variable). A too low atomisation temperature may cause an incomplete volatilisation of the metal studied and, consequently, be responsible for error in iron quantification. On the opposite, a too high atomisation temperature induces a too fast volatilisation of the metal which results in a signal too short to obtain a good quality measurement. So, from literature data and our knowledge of absorption spectrometry the study range for this factor was 2500-2700 °C.

However, the whole experimental domain defined above by the electrothermal factors variations is not accessible: indeed, when the calcination temperature *CT* is set at the lowest level ($E_2 = –1$), a short calcination duration *CD* ($E_3 = –1$) will result in a partial sample calcination and, thus, in a bad measurement. So, by exclusion of this experimental condition we obtained a reduced domain, *i.e.* the worthwhile experimental domain of study. We consequently chose three levels of study for all the factors ($E_i = –1$; $E_i = 0$ and $E_i = +1$) except for the calcination duration to which we added a fourth level at $E_3 = –0.5$ to have an alternative to the following unrealisable combination $E_2 = –1$; $E_3 = –1$. All the levels used for the four experimental factors are given in table I-B.

Experimental responses

We followed three experimental responses Y_i for all of them exert an important influence on the quality of the measurement:

s or Y_1, the standard deviation of the instantaneous specific absorbance without neutral atoms. Indeed, for each measurement this parameter directly quantifies the noise affecting the absorbance;

Q_A *or* Y_2, the specific integrated absorbance is directly proportional to the metal concentration in the sample of concern (Fig. 1).

Q_B *or* Y_3, the non-specific integrated absorbance which corresponds to the absorbance of the metals interfering at the same wavelength: 248.3 nm (Fig. 1).

Finally, to obtain the best measurement conditions, the standard deviation s and the non-specific integrated absorbance Q_B must be minimised; on the other hand, the integrated absorbance Q_A had to be maximised.

Experimental methodology

Mathematical models

The spectroscopic factors investigated consisted of 2 quantitative ones, S_1 and S_3, and a qualitative one, the slit height S_2. However, as this qualitative factor has only two levels it can be described by a linear polynomial mathematical model; indeed, an interpolation between the levels $S_2 = -1$ and $S_2 = +1$ will be a nonsense, but it is always possible to study the interactions with other factors. For the factors where the evolution of the experimental response was known as being non linear, we postulated a classical second-degree mathematical model. Consequently, the evolution of experimental response can be described by using the following particular polynomial model with all the linear terms ($b_i \times S_i$) and all the interaction terms ($b_{ij} \times S_i \times S_j$), but with only two quadratic terms ($b_{ii} \times S_i^2$); it thus contains $p_S = 9$ coefficients:

$$Yi = b_0 + b_1 \times S_1 + b_2 \times S_2 + b_3 \times S_3 + b_{11} \times S_1^2 + b_{33} \times S_3^2 + b_{12} \times S_1 \times S_2 + b_{13} \times S_1 \times S_3 + b_{23} \times S_2 \times S_3.$$

For the study of electrothermal factors we postulated a classical second-degree mathematical model with $p_E = 15$ coefficients b_i to describe the phenomenon evolution.

Building of the D-optimal experimental designs

For the spectroscopic factors, one could eventually determine the coefficients of the particular polynomial model (with three factors and only two quadratic terms) by using an asymmetric fractional factorial design. However, this design may not be the best one because the centre value proposed for $S_3 = 0$ does not correspond to a usable level of study. Consequently, we built a D-optimal experimental design specially dedicated to fit our optimisation problem [7,8].

In this purpose, we first built an asymmetric full factorial design for one 2-level factor, one 3-level factor and one 4-level factor ($2^1.3^1.4^1$) corresponding to 24 experiments plus a centre point. The level of slit width factor was set to the values specifically usable with our apparatus, *i.e.* $S_3 = -1$, –0.778, –0.111 or +1. This matrix, which fits well our experimental domain of study, is the spectroscopic-factor candidate-point matrix ${}^S\xi_N$.

To solve the electrothermal factor model, one can use either a centre composite experimental design or a Doehlert design. But, none of these classical designs could be utilised in our particular experimental domain. So, we had to build a new D-optimal experimental design.

We first built an asymmetric full factorial design for three 3-level factors and one 4-level factor ($3^3.4^1$) in 108 experiments plus a centre point. After removing the 9 unrealisable experimental conditions that simultaneously correspond to $E_2 = -1$ and $E_3 = -1$ we obtained the electrothermal-factor candidate-point matrix ${}^E\xi_N$ in $N = 100$ experiments. This matrix ${}^E\xi_N$ described precisely the worthwhile experimental domain.

For the spectroscopic factors and electrothermal factors we applied the same procedure to build the D-optimal matrix. The numerous subset matrices ξ_n (with $p < n < N$) that can be built from ξ_N constitute the Ξ group. For each number of experiments n we intended to select from Ξ the D-optimal matrix ξ_n^* maximising the determinant of ($\boldsymbol{X'X}$), the information matrix. These D-optimal matrices were made through an iterative maximisation of the determinant value following the Fedorov algorithm whose applications have been described elsewhere [7,8,12].

Selection of a D-optimal experimental design

All the D-optimal matrices obtained by the Fedorov algorithm can be characterised by several quality criteria [10,13], *i.e.* i) the determinant of the matrix of moments $M(\boldsymbol{X})$ that we wish to maximise; ii) the trace of the dispersion matrix $(\boldsymbol{X'X})^{-1}$ to be minimised; iii) the largest variance function $d(x)_{MAX}$ to be also minimised and iv) the G-efficiency to be maximised.

The variations of these criteria in the case of spectroscopic factors *versus* the number of experiments n are depicted in figure 2. The maximum matrix of moments $M(\boldsymbol{X})$ value and a satisfactory trace value are obtained for the 14-experiment D-optimal matrix ${}^S\xi_{14}{}^*$. However, the 12-experiment matrix ${}^S\xi_{12}{}^*$ permits one to obtain a satisfactory value of the largest variance function $d(x)_{MAX}$ below 1; the addition of 2 other experiments does not improve the $d(x)_{MAX}$ value. Consequently, the G-efficiency maximum is obtained with the 12-experiment matrix ${}^S\xi_{12}{}^*$ and decreases when the experiments are more numerous. These results led us to choose the 12-experiment D-optimal matrix ${}^S\xi_{12}{}^*$ presented in table II-A for spectroscopic factors optimisation.

For the electrothermal factors the variations of the quality criteria *versus* the number of experiments n are shown in figure 3, which highlights that, in comparison with the 26-experiment matrix, the 27-experiment D-optimal matrix ${}^E\xi_{27}{}^*$ improves the quality of all criteria. Moreover, a greater number of experiments than 27 does not significantly improve the matrix quality. By the end the ${}^E\xi_{27}{}^*$ matrix has the highest G-efficiency value which corresponds to the best compromise between the quality of the model prediction and the number of experiments to be performed. To optimise the electrothermal factors we, therefore, selected this 27-experiment matrix ${}^E\xi_{27}{}^*$ presented in table III-A.

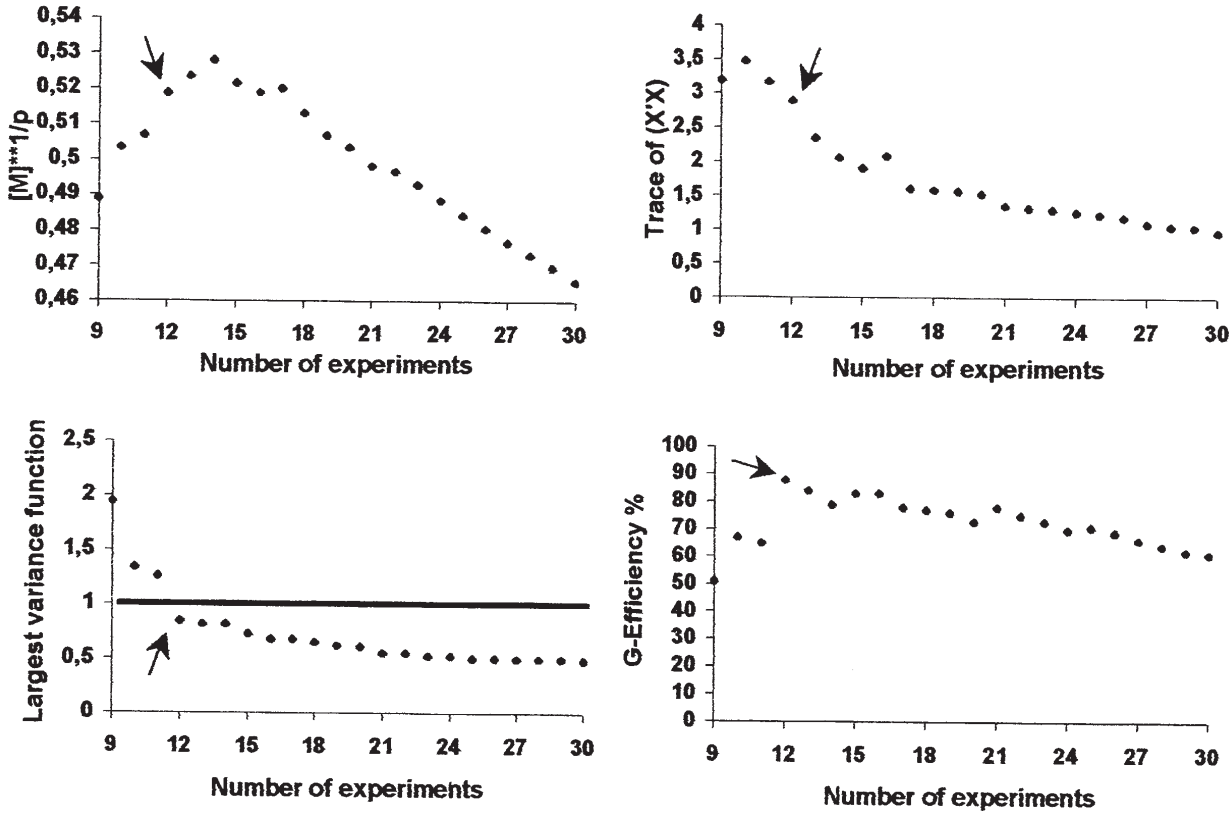

Figure 2. Evolution of quality criteria for the spectroscopic D-Optimal matrix $^{s\varepsilon}\xi_n$* versus the number of experiments *n*.

Table II. Part A: D-optimal spectroscopic experimental matrix into 12 experiments ($^{s\varepsilon}\xi_{12}$*); part B: Experimental responses obtained; part C: computed experimental response.

	Part A: Spectroscopic factors			*Part B: Experimental response*			*Part C: Computed response*
Exp. N°	*C (mA)*	*H*	*W (nm)*	*s × 10³*	*Q_A × 10³*	*Q_B × 10³*	*C_{EILOD} (ng.L⁻¹)*
1	7	Normal	0.1	7.50	27.0	38.0	450
2	15	Normal	0.1	2.50	40.0	46.5	127
3	23	Normal	0.1	2.45	37.0	61.0	140
4	7	Reduced	0.2	5.55	35.0	33.5	274
5	23	Reduced	0.2	1.95	39.0	49.0	107
6	15	Reduced	0.5	1.95	37.0	39.5	108
7	23	Normal	0.5	1.60	40.5	52.0	88
8	7	Reduced	1	4.90	23.0	22.0	337
9	23	Reduced	1	1.40	19.0	49.5	143
10	7	Normal	1	4.10	23.0	26.0	288
11	15	Normal	1	1.60	26.0	48.0	119
12	23	Normal	1	1.45	24.5	43.5	124

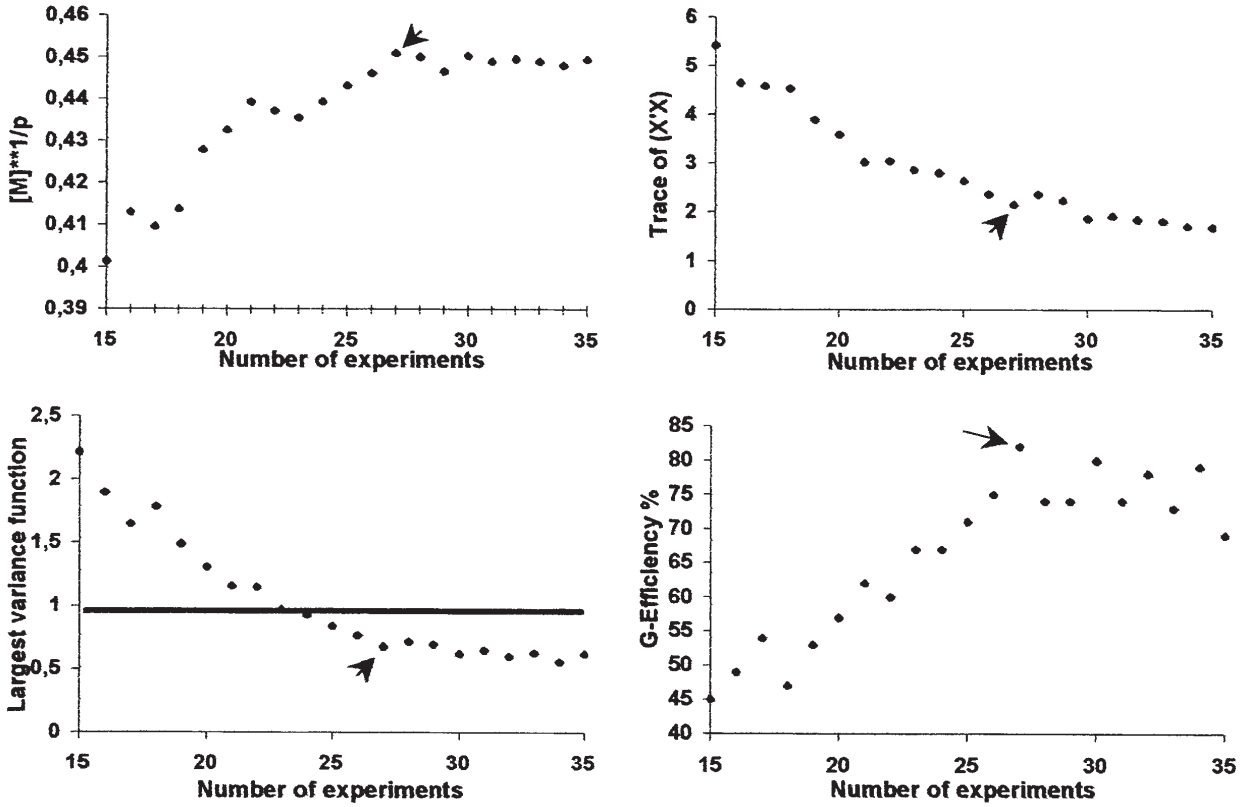

Figure 3. Evolution of quality criteria for the electrothermal D-Optimal matrix $^{E}\xi_n$* *versus* the number of experiments *n*.

In addition, we checked that the inflation factor values of the two D-optimal matrices selected were sufficiently close to 1 to ensure a sufficient precision in the determination of the model coefficients b_i.

From another point of view, the separation of the optimisation procedure into two different parts, the spectroscopic and the electrothermal factors, avoids one to perform more than 60 measurements in a row which could induce a systematic deviation of the experimental responses consecutively to an alteration of the furnace surface.

Experimental results and discussion

Optimisation of experimental responses

Our experimental results are presented in table II-B for the spectroscopic factors and in table III-B for the electrothermal ones. A Box-Cox transformation was used to select the best transformed experimental responses to be studied. The spectroscopic factors followed were $1/\sqrt{s}$, Q_A and Q_B; our aim was to maximise the first two of them and minimise the third one. In the case of electrothermal factors we studied $1/s$, $1/\sqrt{Q_B}$ and $1/Q_A$ with the same aim as previously to maximise the two first ones and that minimise the last one. The mathematical models were then computed and validated through an analysis of variance with an independent estimation of the experimental variance.

For each of the three studied experimental responses we carried out investigations to find the optimum experimental conditions; the results obtained for both the spectroscopic and the electrothermal factors are presented in table IV-A. The optima reached for the electrothermal factors were interesting because of the low values of s ($1.58\ 10^{-3} \pm 0.04\ 10^{-3}$) and Q_B ($40\ 10^{-3} \pm 5\ 10^{-3}$), and of the high value of Q_A ($23\ 10^{-3} \pm 5\ 10^{-3}$).

However, table IV-A clearly shows that the optimal conditions of each experimental response are located in opposed parts of the experimental domain. Consequently, to obtain the optimum operational condition of the apparatus we had to look for the best possible compromise.

Multi-criteria optimisation

To look for such a compromise we made a multi-criteria optimisation from a desirability transformation. For this treatment, each response was transformed into a partial

Table III. Part A: D-optimal electrothermal matrix into 27 experiments ($^{E\xi}_{27}$*); part B: experimental responses obtained; part C: computed experimental response.

	Part A: Electrothermal factors				*Part B: Experimental responses*			*Part C: Computed response*
Exp. N°	*V (µL)*	*CT (°C)*	*CD (s)*	*AT (°C)*	$s \times 10^3$	$Q_A \times 10^3$	$Q_B \times 10^3$	C_{EILOD} *(ng.L^{-1})*
1	12	1600	10	2500	1.47	7.0	66	89
2	12	1500	20	2500	1.55	6.7	83	94
3	12	1700	30	2500	1.57	6.6	43	95
4	12	1500	50	2500	1.58	6.9	44	90
5	12	1700	50	2500	1.66	6.8	45	99
6	12	1700	10	2600	2.12	7.2	51	109
7	12	1700	10	2700	1.64	8.3	60	79
8	12	1500	20	2700	1.62	7.8	84	82
9	12	1600	30	2700	1.59	7.4	53	82
10	12	1500	50	2700	1.59	8.0	59	81
11	12	1700	50	2700	1.61	7.5	53	83
12	24	1700	10	2500	1.80	16.0	82	53
13	24	1500	20	2600	2.07	16.7	94	55
14	24	1600	50	2600	1.98	11.3	61	70
15	24	1600	10	2700	1.62	13.7	68	51
16	24	1700	30	2700	1.58	10.1	57	64
17	36	1700	10	2500	1.82	12.0	43	69
18	36	1500	20	2500	2.11	21.5	232	64
19	36	1600	30	2500	2.06	72.3	255	67
20	36	1500	50	2500	2.05	16.7	70	57
21	36	1700	50	2500	2.02	11.8	51	77
22	36	1600	10	2600	2.09	16.1	144	64
23	36	1700	30	2600	2.09	11.6	85	75
24	36	1700	10	2700	1.63	12.9	98	55
25	36	1500	20	2700	1.64	15.9	132	47
26	36	1500	50	2700	1.64	17.0	121	46
27	36	1700	50	2700	1.69	11.9	114	62

desirability d_i. Each d_i expressed the percentage of satisfaction reached by the experimental response under the different experimental conditions. This means that if the experimental response value is judged as unacceptable by the analyst the d_i value will be set to 0 % of satisfaction; if it is judged as fully satisfactory the d_i value will be set to 100 % of satisfaction indicating that the target has been reached. Between this two extrema an acceptable experimental response will have a d_i value within 0 and 100 %. The threshold values are, of course, subjective and require from the analyst a good knowledge of the technique and of the apparatus. The various thresholds chosen for the optimisation of spectroscopic and electrothermal factors are presented in table V. A left threshold corresponds to an experimental response to be maximised (here Q_A) whereas a right threshold corresponds to an experimental response to be minimised (here s and Q_B). As we had studied the Box-Cox transformation of these responses, ($1/s$; $1/\sqrt{s}$; $1/Q_A$ and $1/\sqrt{Q_B}$) the corresponding thresholds and targets are also reported in table V when necessary.

After the transformation in partial desirability d_i of the three experimental responses, the global desirability D was then obtained by computing the geometric mean using the following equation:

$$D = (d_1 \times d_2 \times d_3)^{1/3}.$$

Figure 4 shows the global desirability of spectroscopic factors *versus* the lamp current and the slit width; since we had observed that the slit height did not exert a significant influence on desirability, it was set to its reduced level. The best compromise was obtained under the following experimental conditions: C = 17 mA, H = Reduced, W = 0.5 nm (Tab. IV-B-upper part) and corresponded to 69 % of global satisfaction by reference to the desirability criteria.

Table IV. Optimal experimental conditions and corresponding optimum responses reached: part A for the three experimental responses; part B for the desirability transformed response; part C for the C_{EILOD} computed experimental response.

	Part A : Experimental responses			*Part B : Desirability*	*Part C : Computed response*
	s (▲)	Q_A (▼)	Q_B (▲)	*D*	C_{EILOD}
Spectroscopic factors					
C (mA)	7	20	21	17	20
H	Reduced	Normal	Normal	Reduced	Reduced
W (nm)	1	0.2	1	0.5	0.5
Corresponding optimum	1.37 ± 0.04 ($\times 10^3$)	41 ± 2 ($\times 10^3$)	24 ± 4 ($\times 10^3$)	69 %	85 ± 5 ($ng.L^{-1}$)
Electrothermal factors					
V (µL)	24	36	12	28	31
CT (°C)	1600	1500	1700	1540	1500
CD (s)	30	10	50	50	50
AT (°C)	2700	2500	2500	2700	2700
Corresponding optimum	1.58 ± 0.04 ($\times 10^3$)	23 ± 5 ($\times 10^3$)	40 ± 5 ($\times 10^3$)	54 %	38 ± 6 ($ng.L^{-1}$)

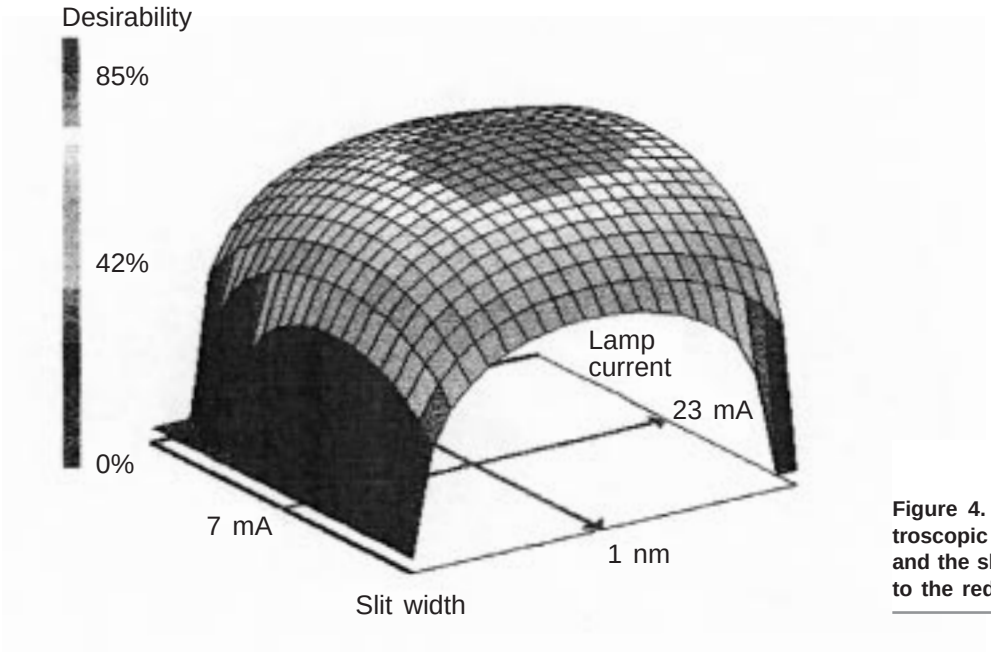

Figure 4. Desirability evolution for the spectroscopic factors versus the lamp current *C* and the slit width *W* (the slit height H was set to the reduced level).

The global desirability of electrothermal factors versus calcination and atomisation temperatures (*V* set to 28 µL and *CD* to 50 s) is displayed on figure 5. The best compromise was obtained under the following conditions *V* = 28 µL; *CT* = 1540 °C, *CD* = 50 s and *AT* = 2700 °C (Table IV-B-lower part) with 54 % of global satisfaction. Under the optimal conditions mentioned above we obtained a low standard deviation *s* of $1.62\ 10^{-3} \pm 0.05\ 10^{-3}$ with a sufficiently high specific absorbance Q_A of $16\ 10^{-3} \pm 2\ 10^{-3}$, and a satisfactory low unspecific absorbance Q_B of $80\ 10^{-3} \pm 10\ 10^{-3}$. These experimental responses corresponded to a very interesting compromise.

Figure 5 shows that, in an opposite part of the experimental domain, there is another satisfactory compromise

Table V. Desirability transformation for the measured experimental responses and for the corresponding Box-Cox transformed experimental responses.

Factors optimisation	*Experimental and transformed responses*	*Partial desirability* d_i *(%)* *0 % (Left threshold)*	*100 % (Target)*	*0 % (Right threshold)*
Spectroscopic	$s \times 10^3$ (▲)		1.1	4.4
	$1 / \sqrt{s}$ (▼)	15	30	
	$Q_A \times 10^3$ (▼)	20	50	
	$Q_B \times 10^3$ (▲)		25	70
Electrothermal	$s \times 10^3$ (▲)		1.40	2.00
	$1 / s$ (▼)	500	700	
	$Q_A \times 10^3$ (▼)	12	25	
	$1 / Q_A$ (▲)		40	80
	$Q_B \times 10^3$ (▲)		35	110
	$1 / \sqrt{Q_B}$ (▼)	3.0	5.3	

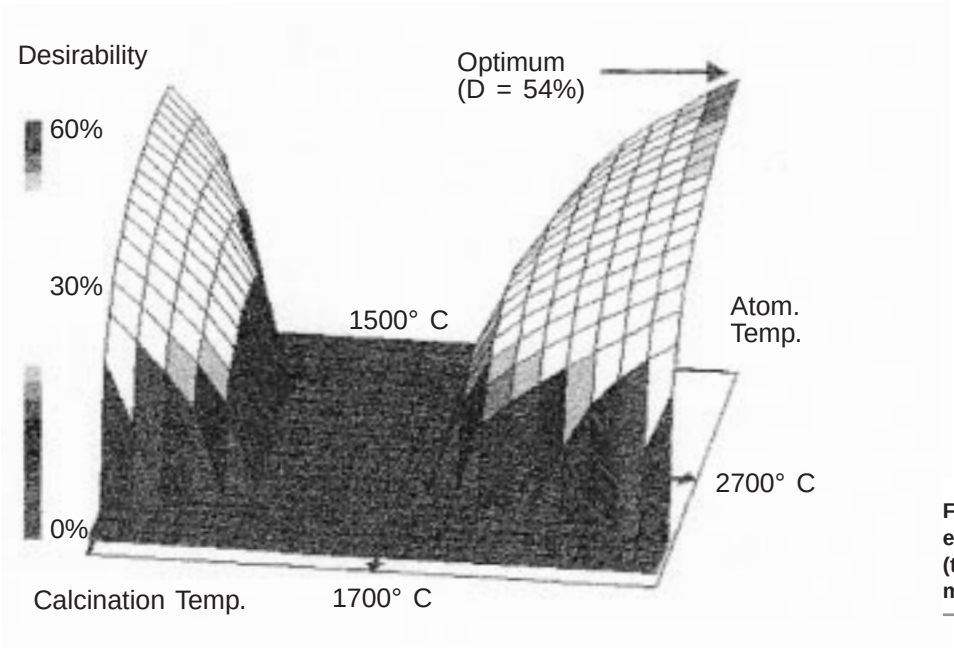

Figure 5. Desirability evolution for the electrothermal factors versus *CT* and *AT* (the other factors were set to their optimum values *i.e: V* = 28 µL; *CD* = 50 s).

with almost 48 % of global desirability; it is obtained with an opposite atomisation temperature *AT* of 2500 °C and a calcination temperature *CT* of 1550 °C. In addition, we also had there interesting values for *s* ($1.87\ 10^{-3} \pm 0.06\ 10^{-3}$), Q_A ($16\ 10^{-3} \pm 10^{-3}$) and Q_B ($60\ 10^{-3} \pm 9\ 10^{-3}$). These two compromises being of similar quality, they give the analyst the choice of experimental conditions.

An analysis of table IV highlights that the best desirability compromises (Part B) are reached under experimental conditions very different from the optima of the three experimental responses (Part A). This remark is valid both for spectroscopic and electrothermal factors (upper part and lower part of table IV, respectively).

Optimisation of the new computed response

If the desirability transformation provides an interesting approach to optimisation problems in electrothermal atomic absorption spectrometry, it, however, requires additional calculation along with experimental knowledge of this technique. So, to simplify the procedure and avoid the use of desirability transformation, we studied a new computed experimental response, that manufacturers should provide

with spectrometer software. We will, consequently, propose to use the Estimated Instrumental Limit of Detection (C_{EILOD}) as optimisation criterion; C_{EILOD} takes into account the sensitivity and noise affecting the integrated absorbance measurements [14]. It can be computed using the following formula and expressed in concentration units:

$$C_{EILOD} = 3s_0 \sqrt{T_s t_{int} \cdot 10^{\tilde{A}_{BG}}} \frac{C}{Q_A}$$

$$\tilde{A}_{BG} = [A_{BG(max)} + Q_B.t_{int}^{-1}]$$

where s, Q_A and Q_B are the experimental responses previously defined, t_{int} is the integration time, C is the iron concentration in seawater sample, T_s is the sampling rate and $A_{BG(max)}$ is the maximum instantaneous absorbance of the non-specific signal. In this formula the C/Q_A ratio gives the measurement sensitivity. As C_{EILOD} corresponds to an estimation of the detection limit expressed in concentration, it must be logically minimised to obtain the optimal operational conditions.

From the experimental results previously reported we computed the fourth experimental response, *i.e.* the C_{EILOD} for the spectroscopic (Tab. IIC) and electrothermal (Tab. IIIC) factors. Following a Box-Cox transformation we studied $1/\sqrt{C_{EILOD}}$ for spectroscopic factors and C_{EILOD} for electrothermal ones. Then, the same type of mathematical model was validated by an analysis of variance with an independent estimation of the experimental variance. The evolution of $1/\sqrt{C_{EILOD}}$ is presented on figure 6 for spectroscopic factors whereas figure 7 shows the evolution of C_{EILOD} for electrothermal factors.

Figure 6 shows that the maximum $1/\sqrt{C_{EILOD}}$ value of 7.36 for the spectroscopic factors corresponds to 85 ± 5 ng.L^{-1} and that C_{EILOD} value can be obtained for a centre slit width with a high lamp current.

In the case of electrothermal factors (Fig. 7) the minimum C_{EILOD} value is obtained for a high atomisation temperature with a low calcination temperature. Under these experimental conditions C_{EILOD} is equal to 38 ± 6 ng.L^{-1} which is interesting because it is a very low value compared to literature data. Like for the desirability study, another acceptable C_{EILOD} value of 55 ± 7 ng.L^{-1} can be obtained at the same calcination temperature, but with an opposite low atomisation value.

A comparison of the results obtained by the desirability study and by the experimental response transformation, Table IV-B and IV-C respectively, clearly show that the optimal experimental conditions proposed were exactly the same. This comment is valid for both the spectroscopic and electrothermal factors (upper part of Tab. IV: C = 17 mA, H = Reduced, W = 0.5 nm and lower part of Tab. IV: V = 31 µL, CT = 1500 °C, CD = 50 s and AT = 2700 °C, respectively). This important result proves the relevance of C_{EILOD} as a mathematical transformation of the experimental responses because it well expresses the quality of experimental measurements. Its expression in simple units of concentration along with its direct calculation make C_{EILOD} a relevant optimisation criterion.

Finally, the experimental responses predicted by the mathematical models under the experimental-condition compromise were verified by conducting new experiments. The results presented in table VI illustrate that all the predicted

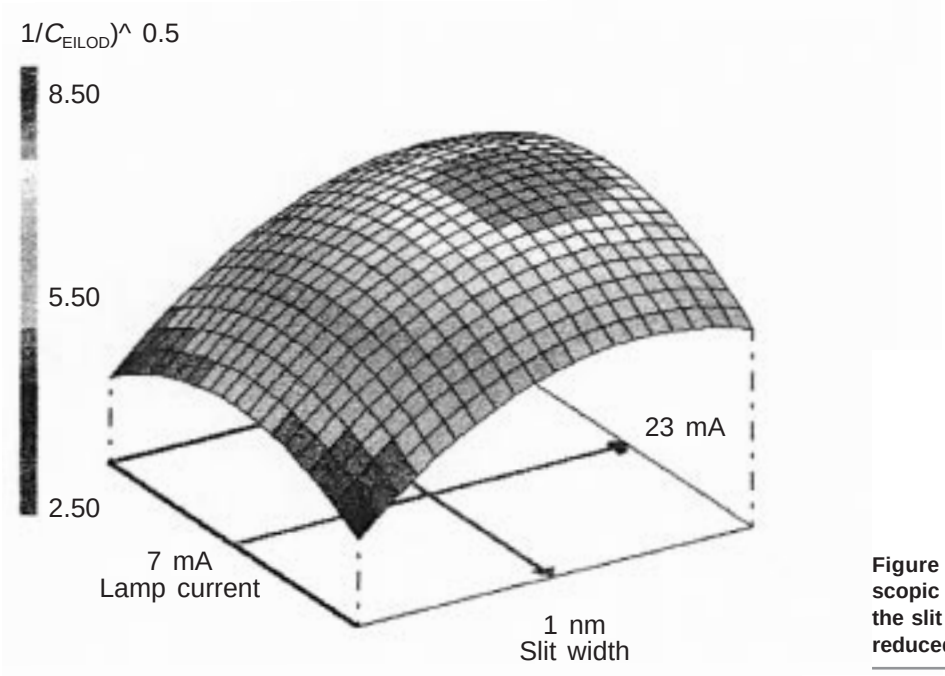

Figure 6. $1/\sqrt{C_{EILOD}}$ evolution for the spectroscopic factors versus the lamp current *C* and the slit width *W* (the slit height H was set to the reduced level).

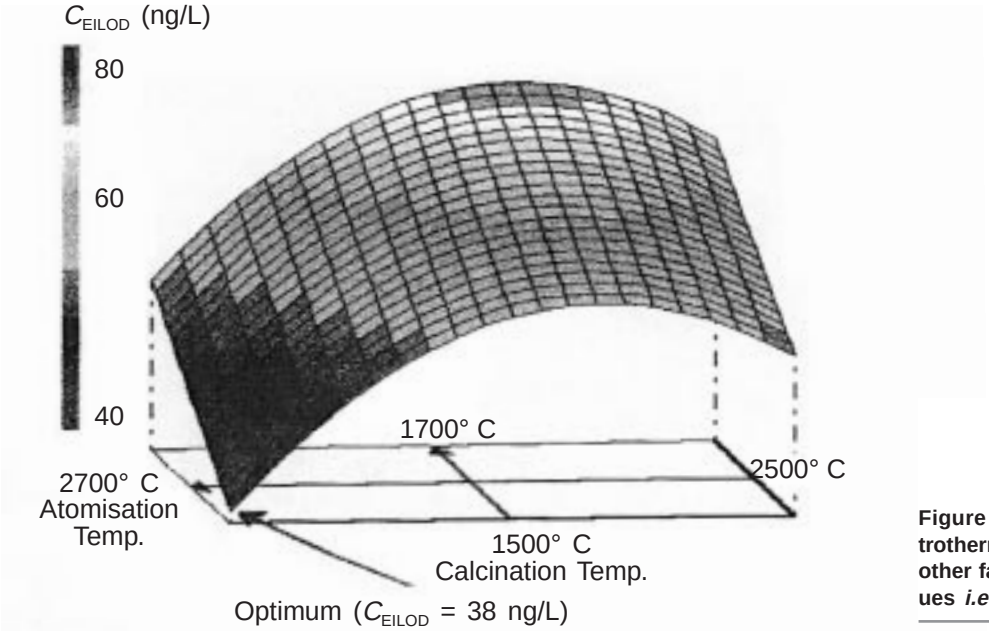

Figure 7. C_{EILOD} evolution for the electrothermal factors *versus* *CT* and *AT* (the other factors were set to their optimum values *i.e:* *V* = 31 µL; *CD* = 50 s).

Table VI. Comparison of the predicted and experimental values under the optimal experimental conditions for spectroscopic factors (Part A) and electrothermal factors (Part B).

Factors	C_{EILOD} *(ng.L^{-1})*	
	Predicted optimum values	*Experimental values*
Spectroscopic	85 ± 5	94 ± 5
Electrothermal	38 ± 6	40 ± 6

C_{EILODs} are comparable to the experimental values within their uncertainty range. This confirms the validity of the two mathematical models used.

Conclusion

This study on iron determination in sea water, near the quantification limit, by electrothermal atomic absorption spectrometry highlighted the importance of experimental methodology in the optimisation of operating conditions. This optimisation of spectroscopic and electrothermal factors achieved by performing a low number of experiments allowed us to reach an estimated detection limit of 40 ng.L^{-1}. We also demonstrated the great interest of the D-optimal matrix construction when the experimental design had to be adapted to a particular experimental domain with constraints.

Moreover, the compromise research illustrated the good agreement of the results obtained after the desirability transformation with those from C_{EILOD} calculation. This proves that the C_{EILOD} computed experimental response is a good criterion to optimise operating conditions in atomic absorption spectrometry. It would be worthwhile if spectrometer manufacturers could integrate the C_{EILOD} calculation function into the spectrometer control software, for it would allow an easier optimisation protocol.

Acknowledgements

The authors wish to thanks Pr. Phan Tan Luu of the Aix-Marseille III University (France) for using the Nemrod-Windows software. They acknowledge to C. Desrues and M.P. Friocourt for they constructive contribution to this work. They acknowledge finally the “Conseil Régional de Bretagne” for it’s financial support.

Appendix

S_i	Spectroscopic experimental factor *i* in coded value
E_i	Electrothermal experimental factor *i* in coded value
W	Slit width (real value, nm).
H	Entrance monochromator slit height (real value, qualitative)
C	Lamp current (real value, mA).
CT	Calcination temperature (real value, °C)
V	Injected volume (real value, µL)
CD	Calcination duration (real value, s)
AT	Atomisation temperature (real value, °C)
Y_i	Experimental responses i
s	Standard deviation of the instantaneous specific absorbance
Q_A	Integrated specific absorbance
Q_B	Non-specific integrated absorbance
t_{int}	Integration time
Ts	Sampling rate
$A_{BG(max)}$	Maximum instantaneous absorbance of the non-specific signal
C_{EILOD}	Estimated instrumental limit of detection
b_i	Models coefficients *i*
p_S ; p_E	Number of coefficients in the spectroscopic or the electrothermal factors models
n	Number of experiments
N	Number of experiments of the candidate-point matrices ${}^S\xi_N$ or ${}^E\xi_N$
Ξ	Set of *n*-experiment matrices that can be built from ξ_N
${}^S\xi_N$; ${}^E\xi_N$	Spectroscopic or electrothermal candidate point matrix in *N* experiments
${}^S\xi_n$; ${}^E\xi_n$	Spectroscopic or electrothermal subset matrix in *n* experiments from Ξ ($p < n < N$)
${}^S\xi_n{}^*$; ${}^E\xi_n{}^*$	Spectroscopic or electrothermal D-optimal matrix in *n* experiments
$(\boldsymbol{X}'\boldsymbol{X})$	Information matrix
$(\boldsymbol{X}'\boldsymbol{X})^{-1}$	Dispersion matrix
$M(\boldsymbol{X})$	Matrix of moments
$d(x)_{MAX}$	The largest variance function
d_i	Partial desirability
D	Global desirability

References

1. Stalikas, C.D.; Pilidis, G.A.; Karayannis, M.I. *J. Atomic Absorption Spectrometry* **1996**, *11*, 595.
2. Kpch, I.; Harrington, C.F.; Reimer, K.J.; Cullen, W.R. *Talanta* **1997**, *44*, 1241.
3. Slaveykova, V.I.; Hoenig, M. *Analyst* **1997**, *122*, 337.
4. Araujo, P.W.; Gomez, M.J.; Mercano, E.; De Benzo, Z.A. *Fresenius' J. Anal. Chem*. **1995**, *351*, 204.
5. Castera, A.; Lacoste, F.; Lespagne, J. *Analusis* **1992**, *20*, 19.
6. Lelièvre, C.; Hennequin, D.; Barillier, D.; Lemasson, F. *Analusis* **1996**, *24*, 39.
7. Araujo, P.W.; Gomez, M.J.; De Benzo, Z.A.; Castillo, C. *Chemom. Intell. Lab. Systems* **1992**, *16*, 203.
8. Gazquez, D.; Sanchez-Vinãs, M.; Gracia-Bagur, M.; Garcia, G. *J. Atomic Absorption Spectrometry* **1998**, *13*, 105.
9. Le Garrec, H.; Giamarchi, P.; Cabon, J.Y.; Le Bihan, A. *Analytica Chimica Acta* **1997,** *350*, 171.
10. Le Garrec, H.; Giamarchi, P.; Cabon, J.Y.; Le Bihan, A. *Analytica Chimica Acta* **1998,** *350*, 59.
11. Matthieu, D.; Phan Tan Luu, R. NEMROD-W Software, Aix-Marseille III University (France), 1999.
12. De Aguiar, P.F.; Bourguignon, B.; Khots, M.S.; Massart, D.L.; Phan Tan Luu, R. *Chemometrics Intelligent Laboratory Systems* **1995**, *30*, 199.
13. Sergent, M.; Mathieu, D.; Phan Tan Luu, R.; Drava, G. *Chemometrics Intelligent Laboratory Systems* **1995**, *27*, 153.
14. Le Bihan, A.; Le Garrec, H.; Cabon, J.Y.; Guern, Y. *J. Anal. At. Spectrom*. **1995,** *10*, 993.